



HAL
open science

Coupling geochemical and biological approaches to assess the availability of cadmium in freshwater sediment

A. Dabrin, C. Durand, J. Garric, Olivier Geffard, B.J.D. Ferrari, Marina Coquery

► **To cite this version:**

A. Dabrin, C. Durand, J. Garric, Olivier Geffard, B.J.D. Ferrari, et al.. Coupling geochemical and biological approaches to assess the availability of cadmium in freshwater sediment. *Science of the Total Environment*, 2012, 424, p. 308 - p. 315. 10.1016/j.scitotenv.2012.02.069 . hal-00715728

HAL Id: hal-00715728

<https://hal.science/hal-00715728v1>

Submitted on 9 Jul 2012

HAL is a multi-disciplinary open access archive for the deposit and dissemination of scientific research documents, whether they are published or not. The documents may come from teaching and research institutions in France or abroad, or from public or private research centers.

L'archive ouverte pluridisciplinaire **HAL**, est destinée au dépôt et à la diffusion de documents scientifiques de niveau recherche, publiés ou non, émanant des établissements d'enseignement et de recherche français ou étrangers, des laboratoires publics ou privés.

1 Coupling geochemical and biological approaches to assess the
2 availability of cadmium in freshwater sediment

3
4 Aymeric Dabrin, Cyrielle L. Durand, Jeanne Garric, Olivier Geffard, Benoit J.D. Ferrari,
5 Marina Coquery

6
7 Cemagref, UR MALY, 3bis quai Chauveau, CP 220, F-69336 Lyon, France

8 Corresponding author: phone: +33 4 72 20 89 33

9 aymeric.dabrin@cemagref.fr

10

11 **Abstract**

12

13 Sediments are considered as a sink for metals, and the assessment of metal bioavailability for
14 benthic organisms represents a great challenge. Diffusive Gradient in Thin films (DGT),
15 developed to measure labile metals in aquatic media, have more recently been applied to
16 sediment. Nevertheless, few studies have determined the relation between measurements from
17 DGT and bioaccumulation in different benthic organisms. The aim of our work was to
18 determine if labile metal measured by DGT in sediment is representative of bioavailable
19 metal for benthic organisms. We focused our work on Cd and chose to use the diversity of
20 ecological traits from different organisms to better understand the measurement given by
21 DGT. We exposed simultaneously DGT and 3 macroinvertebrates species (the chironomid, *C.*
22 *riparius*; the amphipod, *G. fossarum*; the mudsnail, *P. antipodarum*) to a natural sediment Cd-
23 spiked at environmental relevant concentrations. The nature of sediment-bound Cd was also
24 determined by means of sequential extractions in order to better interpret DGT measurements.
25 Cadmium concentrations were determined in DGT and in the 3 organisms after one week of
26 exposure. Results provided by DGT indicated that Cd was poorly released from particulate
27 phase to pore water, suggesting that Cd measured by DGT was representative of the pore
28 waters labile fraction. Sequential extractions showed that the percentage of Cd bound to
29 carbonate fraction increased simultaneously with Cd-spiking level; hence, this Cd fraction
30 was poorly reactive to supply DGT demand. Cadmium accumulation rates were similar
31 between DGT measurements and *P. antipodarum*, suggesting that labile Cd in pore waters
32 was representative of bioavailable Cd for this species. Cadmium accumulation rates in *C.*
33 *riparius* were higher than in DGT, demonstrating that *C. riparius* can mobilize Cd bound to
34 carbonate phase. *G. fossarum* showed the lowest Cd accumulation rates, suggesting that they
35 were mainly exposed to Cd from overlaying waters.

36

37 Keywords: spiked-sediment, cadmium, DGT, sequential extractions, bioaccumulation,
38 macroinvertebrates, ecological traits

39

40

41 **1. Introduction**

42
43 Sediment is generally considered as an important compartment to be investigated for
44 evaluating the ecological integrity of an aquatic ecosystem. It provides a habitat for a large
45 diversity of communities, but also serves as a reservoir for many pollutants. Sediment
46 contamination primarily occurs via hydrodynamic processes during which many pollutants
47 present in water are readily adsorbed on colloids that can aggregate with each other and settle
48 to the bottom of aquatic systems (Buffle et al., 1998; Vignati et al., 2005). Once in sediment,
49 the evaluation of pollutants mobility and bioavailability remains difficult because of the
50 complex interactions between their own intrinsic properties, the geochemical/climatic factors
51 and the biodiversity on-place (Munkittrick and McCarty, 1995; Chapman et al., 2003). In
52 particular, the lability and the bioavailability of trace metals in sediments are function of the
53 targeted metal, its colloidal, dissolved and particulate partition, its speciation, sediment
54 physico-chemical characteristics (i.e., porosity, grain size, organic matter content), redox and
55 pH conditions, and the physiological and ecological characteristics of the exposed organisms.
56 Traditionally, the assessment of metal availability in sediments using a geochemical approach
57 includes measurements of metals in dissolved and particulate phases and chemical extractions
58 of available fractions (Tessier et al., 1979; Buykx et al., 2000). However, the total metal
59 concentration in sediments is generally not a good proxy to predict bioaccumulation or
60 biological effects (Di Toro et al., 1992). It was demonstrated in several case studies that pore
61 waters metal concentration was a better tool to assess metal bioavailability in sediment (Di
62 Toro et al., 1992; Ankley et al., 1993a; Berry et al., 1996); nonetheless, pore waters metal
63 concentration did not reflect the supply of metals from the particulate phase when particles
64 are ingested by organisms, such as chironomids larvae (Bervoets et al., 1997; Warren et al.,
65 1998). Another parameter which strongly controls metal mobility in sediments is the acid-
66 volatile sulphides (AVS). Acid-volatile sulphides are known to bind trace metals (i.e., Cd, Cu,
67 Ni, Pb and Zn) in marine or freshwater sediments, resulting in insoluble sulphides complexes
68 which reduce metal mobility and toxicity (Di Toro et al., 1992; Ankley et al., 1993b; Ankley
69 et al., 1996; Burton et al., 2005). However, the AVS model did not support the prediction of
70 metals bioaccumulation in benthic organisms for heavily contaminated freshwater sediments
71 (Ankley, 1996; Warren et al., 1998; Lee et al., 2000; De Jonge et al., 2009). More recently,
72 the Diffusive Gradient in Thin films (DGT), initially developed in the 1990's to measure
73 labile metals in surface waters (Zhang and Davison, 1995), has been applied to soil and
74 sediment (Harper et al., 2000; Zhang and Davison, 2000; Zhang et al., 2004; Rachou et al.,

75 2007). When a DGT is introduced into sediments, trace metals of the pore waters are rapidly
76 bound by the resin of the device; this results in a decrease of pore waters trace metals
77 concentrations, inducing a variable resupply from the particulate phase (Zhang et al., 1995).
78 Metal accumulation in DGT and in terrestrial plants has been successfully compared because
79 it operates similarly to active transport across a cell membrane (Zhang et al., 2001; Almås et
80 al., 2006). The comparison is more difficult with benthic organisms, since metal transfer
81 pathways are more complex, involving dissolved, colloidal and also particulate forms when
82 sediment is ingested.

83 The aim of our study was to determine if the measurement of the labile Cd fraction in
84 freshwater sediment using the DGT device is representative of the metallic bioavailable
85 fraction for benthic organisms. We chose to use the diversity of ecological traits and habitats
86 from different organisms to better understand the measurement given by the DGT tool in term
87 of bioavailability. *Chironomus riparius* (insect larvae) are a relevant indicator of metal
88 bioaccumulation because they live within the sediment during their larvae development and a
89 large part of the metals they accumulate comes from the particulate phase due to particles
90 ingestion (Bervoets et al., 1997; Warren et al., 1998). *Gammarus fossarum* (amphipod) and
91 *Potamopyrgus antipodarum* (mudsnail) have been used in ecotoxicological test, especially for
92 the evaluation of metals exposure from the water column (Geffard et al., 2010; Gust et al.,
93 2011), and they have also been recently used to assess sediment toxicity (Mazurová et al.,
94 2008; Mazurová et al., 2010; Schmitt et al., 2010). *G. fossarum* are epibenthic organisms
95 living at the sediment-water interface; hence, they are mostly influenced by metals from the
96 overlying waters. In contrast, *P. antipodarum* are known to live at the sediment-water
97 interface and as well within the first millimeters depth of the sediment (Michaut, 1968); so
98 they are also exposed to metals from pore waters. The nature of sediment-bound Cd was
99 determined by means of sequential extractions in order to better interpret DGT measurements.
100 Therefore, we performed the following laboratory tests under controlled conditions: parallel
101 experiments were conducted by coupling DGT measurements with bioaccumulation
102 measurements on *C. riparius*, *G. fossarum* and *P. antipodarum*. Since several physico-
103 chemical parameters (AVS concentration, organic matter concentration, carbonates...) could
104 induce a variability of geochemical and ecotoxicological results, we decided to use a unique
105 low contaminated natural sediment, Cd-spiked at environmentally relevant concentrations.

106

107 **2. Material and methods**

108

109 2.1 Sediment sampling and Cd spiking

110

111 The sediment used in this study (PG) was collected in October 2009 from the Ain River
112 which is a tributary of the Rhône River in the Southeast of France (N 45°809; E 5°209). This
113 sediment was chosen since concentrations of inorganic (Table 1) and organic contaminants
114 were low and under Threshold Effect Concentrations (TEC; Mc Donald et al., 2000). Surface
115 sediment (10 cm) was sampled using a Van Veen grab (Hydrobios, GmbH), then it was
116 immediately sieved through a 2 mm mesh. It was kept at 4°C before experiments. Five
117 environmentally relevant nominal spiking Cd concentrations (0.5, 1.3, 3.1, 7.8 and
118 19.5 mg kg⁻¹ dry weight) were defined in order to cover a concentration range evenly spread
119 between the Threshold Effect Concentration (TEC; 0.99 mg kg⁻¹) and the Probable Effect
120 Concentration (PEC; 4.98 mg kg⁻¹) defined by Mc Donald et al. (2000). A Control was
121 prepared in the same way as the spiked concentrations. Cadmium spiking (CdCl₂ salts) was
122 realised by mixing wet sediment with the spiked solution using a liquid-solid ratio of 3.6. The
123 water (FOS) used to proceed to the spiking mixing step corresponded to a spring-water
124 adjusted to 300 µS cm⁻¹ with purified water. The composition and characteristics of this water
125 were regularly checked during experimental protocol. The pH was circa 6.9; Ca²⁺ and Mg²⁺
126 concentrations averaged 35 mg L⁻¹ and 2.3 mg L⁻¹, respectively. Dissolved cadmium
127 concentrations were below the limit of quantification (LQ = 0.01 µg L⁻¹). The content was
128 mixed on a rotating wheel for 6 hours. After particles settling (48 hours), the supernatant
129 water was removed using a vacuum pump and the sediment was homogenized with a plastic
130 spoon prior to its introduction in test beakers. The same procedure was used for the Control
131 sediment, but with Cd-free FOS water.

132

133 2.2 Experimental protocol

134

135 Subsamples of 100 ml of homogenized spiked sediment were distributed in 500 ml
136 polypropylene beakers. An amount of 400 ml of FOS water was slowly added over the
137 sediment minimising the suspension of the sediment. All beakers were placed in temperature
138 regulated water baths at 21 ± 0.5 C, except for *G. fossarum* (12 ± 1°C), and with a 16:8 h
139 artificial light:dark photoperiod. In order to equilibrate, systems were maintained during 10
140 days before introduction of DGT and organisms. Each beaker was continuously supplied with
141 FOS water using a flow through system to obtain 4 renewals of overlaying waters per day.

142

143 2.3 DGT preparation

144

145 The DGT probe consists in a plastic piston loaded with a diffusive gel layer backed by an ion-
146 exchange resin gel (Chelex 100) and a plastic cap with a 2 cm diameter window. A protective
147 0.45 μm cellulose nitrate filter (0.13 mm thickness, Millipore) separates the diffusive gel from
148 the solution. Diffuse gels (0.8 mm thickness) and resin gels were purchased from DGT
149 Research Ltd (Lancaster, UK). In order to prevent introduction of oxygen during the
150 deployment within the sediment, DGT probes were deoxygenated by immersion in a
151 suspension of 5 g L⁻¹ of Chelex-100 resin (Sigma) in 0.01 M NaCl, bubbled with nitrogen
152 during 24 hours. Before their deployment into the sediment, the probes were transferred in a
153 glove box under nitrogen atmosphere, put in clean plastic jars which were immediately
154 sealed. The probes were exposed to air and oxygenated water only for a few seconds before
155 the insertion into the sediment.

156

157 2.4 Geochemical approach

158

159 Geochemical experiments were only realised for the Control and for the 3 highest
160 concentrations. DGT probes were introduced in the sediment (one DGT per beaker) by
161 pressing them carefully at the sediment-water boundary layer with a polypropylene stick. The
162 window of measurement of the DGT was positioned at a sediment depth of about 1 cm. DGT
163 devices were retrieved at 2, 4, 8, 12, 24, 48, 72 and 144 hours of deployment (except at 2 and
164 4 hours for the Control sediment). One replicate was used at each time for the Control
165 sediment and two replicates were retrieved for the Cd-spiked sediments at 4, 12, 24 and 144
166 hours. After removal, the DGT probes were thoroughly rinsed with MilliQ water and stored at
167 4°C into clean plastic bags. DGT resin gels were eluted with 2.5 ml of 1 M HNO₃ (Merck,
168 Suprapur) into acid-cleaned polypropylene tubes. At the start and at the end of the DGT
169 deployment period, pore waters were extracted from beakers by centrifugation (10 000 g,
170 30 min) and filtration (0.45 μm) under nitrogen atmosphere. Additionally, surface waters
171 were sampled and filtered (0.45 μm) in duplicate at the start of the experiment. At the end of
172 the deployment time, an aliquot of each sediment was sampled under nitrogen conditions and
173 immediately kept at 4°C for sequential extractions and at -19°C for AVS extraction.

174

175 2.5 Bioaccumulation approach

176

177 *C. riparius* were obtained from the laboratory culture. *G. fossarum* and *P. antipodarum* were
178 collected from natural populations in the Bourbre River and the Rhône River (France),
179 respectively. The 3 test organisms were exposed to the Control sediment and to the 4
180 concentrations of Cd-spiked sediments in separate beakers from DGT exposure.

181 Cadmium bioaccumulation was measured on 3 replicate organisms pools (from 3 independent
182 beakers) at the beginning and after 7 days (*C. riparius*, *G. fossarum*) or 10 days (*P.*
183 *antipodarum*) of exposure. Depending on the mortality rates, 35 unshelled *P. antipodarum*
184 (average of 0.033 g d.w.) , 10 *C. riparius* (average of 0.005 g d.w.) and 10 *G. fossarum*
185 (average of 0.050 g d.w.) were retrieved for each replicate pool sample. All the organisms
186 were thoroughly rinsed successively with FOS water, EDTA (3 mM L⁻¹, diluted in FOS
187 water) and FOS water. The replicates were then freeze-dried (-20°C) before analysis.

188

189 2.6 Physico-chemical analyses

190

191 Sediment granulometry was determined using a Coulter LS-100. Acid-volatile sulfides (AVS)
192 were determined on wet sediments using the procedure developed by Allen et al. (1993) and
193 the limit of quantification was 0.12 µmol g⁻¹. Carbonates content was determined by addition
194 of cold HCl to sediment and by measurement of liberated CO₂ volume. Loss on ignition (LOI)
195 was realised by weighting sediment before and after heating at 500°C in order to estimate
196 total organic matter content. In order to better assess the partitioning of Cd among the
197 different carrier phases of the sediment, sequential extractions were realised according to
198 Roulier et al. (2010). In order to preserve the sub-anoxic conditions in the sediment,
199 sequential extractions procedure was realised under nitrogen atmosphere in a box glove using
200 extractants previously deoxygenated. Duplicate samples were run throughout the procedure.
201 To assess the percentage of recovery of the sequential extractions procedure, the bulk
202 sediment was also mineralized with *aqua regia* (HNO₃: HCl, 3:1) using a microwave oven
203 (MARS-5, CEM).

204 Organisms were mineralized with 2 mL of HNO₃ (Suprapur, 65%) using a microwave oven
205 (MARS-5, CEM). Metal concentrations in surface waters, pore waters, DGT eluates,
206 sediments extracts from sequential extractions and in biological samples were analysed by
207 inductively coupled plasma mass spectrometry (ICP-MS, Thermo X7 series^{II}). Blanks and
208 certified reference materials (TM-28.3, lake water, Environment Canada; IAEA-158, marine
209 sediment; NRCC, TORT-2, lobster hepatopancreas) were systematically used to control
210 analytical accuracy and precision. For sediment, typical expanded uncertainties (i.e., 95%

211 confidence intervals) were 5%. Relative standard deviations of Cd concentration for triplicate
212 biological samples ranged between 6 and 38% for *G. fossarum*, between 1 and 13% for *P.*
213 *antipodarum* and between 26 and 52% for *C. riparius*.

214

215 2.7 Data analysis

216

217 The flux of metals from sediment to the DGT device (F_{DGT}) provides information on the
218 ability of the solid phase to resupply the pore waters. F_{DGT} was calculated as follows:

219

$$220 \quad F_{DGT} = \frac{M}{A \times t} \quad (1)$$

221

222 Where M is the accumulated mass of Cd for a resin surface A (cm^2), over the deployment
223 time t (s). The time-averaged concentration at the interface of the sediment and the diffusive
224 gel, C_{DGT} (in $\mu\text{g l}^{-1}$) was calculated as follows (Eq. 2), with D corresponding to the diffusive
225 coefficient of the free metal ion ($\text{cm}^2 \text{s}^{-1}$) in the diffusive layer of thickness Δg (cm):

$$226 \quad C_{DGT} = \frac{M \times \Delta g}{D \times t \times A} \quad (2)$$

227 C_{DGT} generally decreases during the deployment time because the pore waters concentration
228 near the DGT probe progressively decreases. The R ratio, which corresponds to the ratio
229 between C_{DGT} and the initial metal concentration in pore waters (C_{pw}) before the introduction
230 of the DGT probes (Eq. 3), gives an indication of the depletion at the DGT interface (Harper
231 et al., 2000):

$$232 \quad R = \frac{C_{DGT}}{C_{pw}} \quad (3)$$

233 R can be simulated with the 2D-DIFS model (DGT-induced flux in soils) proposed by
234 Sochaczewski et al. (2007). This model is based upon solute exchange between solid phase
235 and pore waters, coupled to diffusion supply of metal to the interface and across the diffusion
236 layer to the resin gel. DIFS-2D was used by fitting experimental values of R over time
237 allowing to derive the parameters conditioning the response of the metal release from the
238 sediment: the size of the particulate labile pool defined by the distribution coefficient K_{dl}
239 (L kg^{-1}) and the characteristic response time (T_c) of the assumed 1st order reversible exchange
240 process between dissolved and solid phases.

241

242 3. Results

243

244 3.1 Geochemical approaches

245

246 Physico-chemical characteristics and particulate metal concentrations of the studied sediment
247 are presented in Table 1. The sediment showed a relatively fine composition since 70% of
248 particles are represented by silts and clays ($< 63 \mu\text{m}$). Acid volatil sulfides concentrations in
249 the sediment were similar between the Control sediment and spiked sediments, with a mean
250 concentration of $8.1 \pm 0.5 \mu\text{mol g}^{-1}$. Calcium carbonates were the main component of the
251 sediment (54%). Particulate trace metal concentrations (Cd, Cr, Ni, Cu, Zn, As and Pb) were
252 low and all below the TEC. Particulate Cd concentrations obtained for the 5 Cd-spiked
253 concentrations were close to the nominal ones, respectively 0.71, 1.35, 2.97, 6.97 and
254 17.5 mg kg^{-1} . Dissolved Cd concentrations in overlaying waters were below the limit of
255 quantification ($0.010 \mu\text{g L}^{-1}$) in beakers containing the Control sediment and the 2 lowest Cd-
256 spiked concentrations. Cadmium concentrations in overlaying waters increased with Cd
257 spiking concentrations, with 0.014, 0.020 and $0.035 \mu\text{g L}^{-1}$ for PG3.1, PG7.8 and PG19.5,
258 respectively. Cadmium pore waters concentrations ranged between $0.02 \mu\text{g L}^{-1}$ (Control
259 sediment) and $1.82 \mu\text{g L}^{-1}$ (PG19.5). Only for PG19.5, Cd pore waters concentrations
260 increased at the end of the experiment ($4.19 \mu\text{g L}^{-1}$). For the other sediments, Cd pore waters
261 concentrations were similar between the start (T0) and the end (T1: 144 hours) of the
262 experiment. The mass of Cd accumulated by the DGT from the Control sediment was too low
263 to be detected in the eluates ($< 0.010 \mu\text{g L}^{-1}$). In contrast, for PG3.1, PG7.8 and PG19.5 Cd-
264 spiked sediments, the mass of Cd trapped by the DGT increased with time up to 48 hours,
265 then remained constant (Figure 1a). Cadmium fluxes through DGT rapidly decreased to reach
266 low and similar values for the 3 highest spiked sediments (Cd fluxes = $0.18 \cdot 10^{-5} \pm 0.10 \text{ ng cm}^{-2}$
267 s^{-1}) after 144 hours of deployment (Figure 1b).

268 Experimental R data, obtained from the ratio between C_{DGT} and the initial pore waters
269 concentrations (Equation 3), were fitted from inverse 2D-DIFS modelling, which allowed to
270 estimate the range of the partition coefficient of the particulate labile Cd pool (K_{dl}) and the
271 response time of the sorption processes (T_c) for the 3 highest Cd-spiked sediments (Table 2).
272 The response times of sorption processes were relatively high ($34 \text{ s} < T_c < 12500 \text{ s}$) and the
273 labile partition coefficients (K_{dl}) very low (< 2.79). The distribution of particulate Cd
274 concentrations obtained by sequential extractions showed that Cd was not present under
275 exchangeable form (F1) or bound to the residual phase (F5) whatever the level of Cd spiking

276 (Figure 2a). Particulate Cd concentrations in F2, F3 and F4 fractions increased with the level
277 of Cd-spiking (Figure 2a), reaching up to 9.34, 5.77 and 1.94 mg kg⁻¹ respectively, for the
278 highest level of spiking (PG19.5). The relative contribution of each fraction (Figure 2b)
279 showed a progressive increase of F2 fraction from 16% (Control) to 54% (PG19.5), at the
280 expense of F3 and F4 fractions, which decreased from 54% to 34% and from 30% to 11%,
281 respectively.

282

283 3.2 Cd bioaccumulation

284

285 Internalised Cd bioaccumulation for *C. riparius*, *G. fossarum* and *P. antipodarum* are reported
286 in Table 3. Since exposure time was different between the tested organisms and in order to
287 compare results, we calculated Cd bioaccumulation rates (Figure 3). Cadmium
288 bioaccumulation rates were the highest in *C. riparius*, ranging from 0.051 ± 0.019 µg g⁻¹ day⁻¹
289 for the Control sediment to 3.68 ± 1.92 µg g⁻¹ day⁻¹ for PG19.5. Cadmium bioaccumulation
290 rates ranged between 0.018 ± 0.007 µg g⁻¹ day⁻¹ and 0.195 ± 0.040 µg g⁻¹ day⁻¹ for *G.*
291 *fossarum* and between 0.060 ± 0.039 µg g⁻¹ day⁻¹ and 0.393 ± 0.008 µg g⁻¹ day⁻¹ for *P.*
292 *antipodarum*, depending on exposure concentration.

293

294 4. Discussion

295

296 4.1 Supply of Cd from the particulate phase

297

298 For the 3 highest Cd-spiked sediments, the mass of Cd trapped by the DGT after 144 hours of
299 deployment was 1.3 times higher between PG3.1 and PG7.8 and 2.0 times higher between
300 PG7.8 and PG19.5. Since total particulate Cd concentrations were about 2.5 times higher
301 between each studied sediment, this suggests that DGT measurement did not reflect the
302 particulate Cd concentrations. Cadmium fluxes towards DGT as a function of time (Figure
303 1b) showed a typical distribution, corresponding to a rapid decrease during the first hours of
304 deployment followed by a plateau. This distribution reflects a consumption of Cd from pore
305 waters and a poor resupply from particles. In contrast, results obtained by Roulier et al. (2010)
306 on natural sediments, exposed in similar conditions, showed an increase of Cd fluxes between
307 48 and 72 h followed by a decrease. The authors proposed that the increase of Cd fluxes was
308 linked to Mn and Fe oxides reduction at the DGT/sediment interface. They obtained Cd fluxes
309 ranging from ~0.1 to 0.7 10⁻⁵ ng cm⁻² s⁻¹ between 24 and 144 h, corresponding to particulate

310 Cd concentrations of 1.4 to 1.8 mg kg⁻¹. In our experiment, despite Cd particulate
311 concentrations reaching up to 17.5 mg kg⁻¹, Cd fluxes were similar, ranging from 0.1 to
312 1.2 10⁻⁵ ng cm⁻² s⁻¹. Moreover, the total mass of Cd was mainly trapped by DGT during the
313 first 24 hours of deployment (38%: PG3.1; 74%: PG7.8; 71%: PG19.5). This suggests that Cd
314 trapped by DGT mainly originated from the pore waters.

315 Pore waters Cd concentrations include all the metal phases (colloidal forms, inert and labile
316 complexes, free ions), while DGT measures only free ions and labile metal. Although few
317 data are available on Cd partition between colloidal and truly dissolved phase in sediment, Cd
318 is known to be poorly present in colloidal complexes in surface waters (Sañudo-Wilhelmy et
319 al., 2002). In our study, we analysed pore waters Cd concentrations at the start and at the end
320 of the DGT deployment. Relative percent deviation (RPD) was below 10% for PG3.1 and
321 PG7.8, showing a good reproducibility between beakers and that equilibration steady state
322 was reached at the onset of the experiment. However, a large difference was noted for PG19.5
323 (RPD = 79%). This indicates an evolution of the sediment at high Cd-spiked level, probably
324 due to a pH decrease (Hutchins et al., 2007). Indeed, metal-spiking might result in a drop of
325 pH in relation with (i) hydrolysis of metal-spiked (ii) oxidative precipitation of Fe in pore
326 waters and (iii) competition between protons H⁺ and metal-spiked for particulate sorption
327 sites.

328 Nonetheless the plot of experimental R ratio calculated for PG19.5 using initial and final pore
329 waters concentrations showed very similar distributions (Figure 4). Moreover, the R ratio
330 distribution for PG19.5 fitted very well with those of PG3.1 and PG7.8, calculated using
331 means of initial and final pore waters concentrations. The distribution of the R ratio showed a
332 fast decrease during the first 8 hours of DGT deployment, reaching a very small R ratio
333 (< 0.16). Then, the R ratio slowly decreased and stabilized below 0.04 after 144 hours of DGT
334 deployment. Apparently, whatever the level of Cd-spiking, Cd in pore waters was rapidly
335 bound by the DGT in the first hours of deployment, followed by a very low resupply from the
336 particulate phase. Ernstberger et al. (2002) exposed DGT to alluvial soil from 4 hours to 19.5
337 days; the R ratio was about 0.6 at the start of the experiment, then reached about 0.35 after
338 144 hours of deployment. In a similar study, Ernstberger et al. (2005) exposed DGT to 5
339 different soils with similar particulate Cd concentrations (3.24 ± 0.07 mg kg⁻¹), but with
340 variable pH, granulometry and organic carbon content. The R ratios were higher than our
341 results, ranging between ~0.8 and ~0.4 at the start of the experiment, and between ~0.6 and
342 ~0.2 after 144 hours. The highest R ratios were obtained for the clayey soils with neutral pH
343 and organic matter content from 2.6 to 5.8%. We obtained significantly lower R ratio, in spite

344 of high clay ($<63 \mu\text{m} = 70\%$) and high organic carbon content (LOI = 13%). This suggests
345 that in our case, spiked Cd was probably bound to unreactive particulate phases.

346 The 2D-DIFS model was used to model the R ratio distribution in order to determine K_{dl} and
347 T_c parameters. An accurate determination of these two parameters was difficult due to a large
348 number of possible combinations (K_{dl} , T_c) which can fit the experimental data (Lehto et al.,
349 2008). Thus, several response times (T_c) and partition coefficient (K_{dl}) were proposed
350 (Table 2). We obtained very low values for K_{dl} (< 2.79) and high T_c values (ranging between
351 34 and 12500 s) for the 3 highest Cd-spiked sediments. In Roulier et al. (2008), DGT were
352 deployed in 6 polluted sediments and only one couple of K_{dl} (1) and T_c (5000) was
353 comparable to our results. For the other sediments, K_{dl} ranged between 5 and 250,
354 corresponding to small response times (<10 s in most cases). The highest K_{dl} values were
355 obtained for sediments with high organic contents. Similarly, Ernstberger et al. (2005)
356 showed that soils with poor resupply from the particulate phase were sandy and characterised
357 by low pH and low organic matter content. Our tested sediments were fine with relatively
358 high organic matter content (Table 1), but K_{dl} and T_c inferred from the R ratio distributions
359 denoted a poor resupply from the particulate phase.

360 In our study, only total Cd concentration was modified; whatever the level of Cd-spiking,
361 particulate Cd was strongly bound to the particles in response to the equilibrium modification
362 induced by DGT insertion. Acid volatile sulphides are known to strongly bind Cd, reducing
363 its mobility and its toxicity; but AVS concentrations were low in all Cd-spiked sediments
364 ($8.1 \pm 0.5 \mu\text{mol g}^{-1}$; Table 1) and could not explain the equivalent low resupply from
365 particulate phase obtained via DGT.

366 In all tested sediments, Cd was not present in the more potentially mobile particulate phase
367 nor bound to the residual fraction. Cadmium was distributed between the F2, F3 and F4
368 particulate fractions, corresponding to carbonates, Fe and Mn oxides, organic matter and
369 sulfides, respectively (Figure 2). With higher Cd-spiked level, the F2 fraction increased at the
370 expense of F3 and F4 fractions. The significant F2 fraction was due to the high carbonate
371 contents of sediments (54%). Indeed, Cd is known to have a great affinity with carbonates.
372 Thakur et al. (2006) showed that Cd is effectively retained on CaCO_3 by the mechanism of
373 chemisorption at low Cd concentrations, while at higher concentrations, precipitation of
374 CdCO_3 on CaCO_3 surface phase predominated. This phenomenon was also reported in several
375 studies, which showed that Cd was not only bound to sediments by sorption but as well by
376 precipitation of secondary minerals such as otavite (CdCO_3) (Papadopoulos and Rowell,
377 1988; Komárek and Zeman, 2004; Cubillas et al., 2005). In summary, Cd spiked to this highly

378 carbonated sediment was firstly chemisorbed by carbonates surface, followed by CdCO₃
379 precipitation, inducing an exponential increase of the F2 fraction between each spiked
380 sediment. This F2 fraction, presenting a great affinity for Cd, seems to be poorly reactive to
381 supply the decrease of Cd in pore waters induced by the DGT demand.

382

383 4.2 Cd bioavailability

384

385 The slope of the regression between Cd accumulation in organisms, function of total
386 particulate Cd, dissolved Cd in pore waters and in overlaying waters were more pronounced
387 for *C. riparius* as compared to *G. fossarum* and *P. antipodarum* (Figure 3a, b, c), suggesting
388 that *C. riparius* was exposed to a pool of Cd which, in contrast, was not available for the 2
389 others species. By means of in situ experiments, Warren et al. (1998) showed that prediction
390 of Cd concentrations in most benthic animals would be more accurate if they were based on
391 water column rather than on sedimentary Cd concentrations, except for sediment-feeding
392 species such as Chironomids and Tubificidae, which also get Cd from sediments. Indeed, *C.*
393 *riparius* live in close contact with sediments (Young and Harvey, 1991; Charbonneau et al.,
394 1998), burrowing into sediments and creating their own microenvironment by irrigating and
395 ingesting particles. Thus, ligands present in the gut fluid of deposit feeders, provide a
396 complexation capacity for mobilization of sediments-bound metals (Chen et al., 2000).
397 Roulier et al. (2008) reported a significant positive relationship between Cd concentrations in
398 *C. riparius* and particulate Cd concentrations in freshwater contaminated sediments. Our data
399 perfectly fit with this previous study performed under similar exposure conditions (Figure 5).
400 Clearly, these results show that total Cd concentrations in sediments are a good predictor of
401 Cd accumulation in *C. riparius*. Fitting our data with those of Roulier et al. (2008) indicates
402 that particles ingestion by chironomids mobilize more Cd from the particulate phase than
403 DGT. Since sequential extractions showed that Cd-spiked was mainly bound to the carbonate
404 phase, we believe that chironomids are able to assimilate part of the Cd bound to carbonates.
405 To our knowledge, this is the first time that a relationship is established between Cd
406 bioaccumulation in chironomids and a specific Cd particulate fraction. In a similar way,
407 Baumann and Fisher (2011) showed that bioaccumulated Cd in *Nereis Succinea* was related
408 to exchangeable Cd and to Cd bound to the carbonate phase.

409 Cadmium bioaccumulated in *G. fossarum* in the Control sediment (Table 3: 0.12 mg kg⁻¹) was
410 comparable to that obtained (0.28 mg kg⁻¹) in the study of Felten et al. (2008), for the same
411 exposure time in a control solution (Cd < 0.30 µg L⁻¹). Cadmium concentrations in *G.*

412 *fossarum* from the Control sediment, PG0.5 (0.204 mg kg⁻¹) and PG1.3 (0.299 mg kg⁻¹) were
413 in the range of concentrations obtained for organisms collected on the upstream Bourbre
414 River reference site (0.10 to 0.25 mg kg⁻¹), (Geffard et al., 2007). *G. fossarum* showed higher
415 Cd concentration only starting from PG3.1 (0.441 mg kg⁻¹). Since *G. fossarum* are epibenthic
416 species living at the water-sediment interface, they should mainly be influenced by Cd
417 concentrations in overlaying waters. For PG19.5, overlaying waters Cd concentration was
418 0.035 µg L⁻¹ and could explain Cd content in *G. fossarum* (1.37 mg kg⁻¹). In fact, on the
419 Morcille River (Beaujolais region, France), dissolved Cd concentration was about 0.040 µg L⁻¹
420 and Cd concentration in *G. fossarum* averaged 0.80 mg kg⁻¹ (personal communication). If *G.*
421 *fossarum* were exposed to Cd from pore waters (1.82 µg L⁻¹) of PG19.5 sediment, Cd
422 concentrations in *G. fossarum* should have been higher. Indeed, for example, after one week
423 of field exposure at 1 µg L⁻¹, Lacaze et al. (2011) obtained Cd concentrations in *G. fossarum*
424 ranging between 4 and 12 mg kg⁻¹. Pellet et al. (2009) also reported that after one week of
425 laboratory exposure at 1 µg L⁻¹, Cd concentration in *G. fossarum* was about 2.5 mg kg⁻¹.
426 Clearly, all these data strongly support the conclusion that during our experiment, *G.*
427 *fossarum* exposed to Cd-spiked sediment were mainly influenced by Cd present in overlying
428 waters.

429 The slope of Cd bioaccumulation in *P. antipodarum* as a function of particulate Cd
430 concentrations was higher than the slope of Cd bioaccumulation in *G. fossarum* (Figure 3d). It
431 looks like *P. antipodarum* were affected by a pool of Cd that was not seen by *G. fossarum*.
432 Since *P. antipodarum* live at the sediment-water interface and within the first millimeters of
433 the sediment (Michaut, 1968), the exposed organisms were apparently influenced by Cd from
434 pore waters (0.46 to 4.19 µg L⁻¹). However, few data on Cd bioaccumulation in *P.*
435 *antipodarum* are available to reinforce this hypothesis. Gust et al. (2011) showed on a French
436 river with dissolved Cd concentrations of 0.6 µg L⁻¹ that Cd concentrations in *P. antipodarum*
437 were about 1.82 mg kg⁻¹. These data are comparable with Cd concentrations in *P.*
438 *antipodarum* of PG3.1 (1.02 mg kg⁻¹) and PG7.8 (2.12 mg kg⁻¹), corresponding to pore waters
439 Cd concentrations of 0.45 and 1.38 µg L⁻¹.

440 Cadmium accumulation rates in DGT after 144h hours as a function of total particulate
441 concentration showed that the slope of the regression was 2 orders of magnitude lower than
442 the slope obtained for *C. riparius* (Figure 3d). These results corroborates our hypothesis that
443 in a highly carbonated sediment, Cd was not released from the particulate phase to the pore
444 waters in response to the locally depleted dissolved Cd concentration at the DGT-sediment
445 interface, whereas *C. riparius* could bioaccumulate Cd from the particulate phase. Thus, in

446 highly carbonated sediment, DGT is a poor predictor for Cd bioaccumulation in chironomids.
447 This is in accordance with results from Roulier et al. (2008), which did not show a good
448 relationship between Cd bioaccumulated in chironomids and Cd trapped by DGT. For *G.*
449 *fossarum*, the slope of the relationship was lower than the slope for DGT, corroborating the
450 idea that *G. fossarum* exposed to Cd-spiked sediment were mainly influenced by Cd present
451 in overlying waters, while DGT reflected labile Cd from pore waters. Thus, DGT is a poor
452 predictor for Cd bioaccumulation in *G. fossarum* in this highly carbonated sediment.
453 In contrast, the slope of Cd accumulation rates as a function of particulate Cd concentrations
454 was similar between DGT and *P. antipodarum* (Figure 3d). As previously seen, Cd trapped by
455 DGT was represented by labile Cd from pore waters. In conclusion, among the 3 tested
456 species, *P. antipodarum* reflected the best Cd bioavailability from sediment pore waters
457 which was assessed by DGT in this highly carbonated sediment.

458

459 **5. Conclusions**

460

461 Results of our geochemical approach, coupling DGT measurements and sequential
462 extractions, showed that in a highly carbonated sediment, Cd bound to carbonates increased
463 simultaneously with Cd-spiking level and was poorly reactive to supply the decrease of Cd in
464 pore waters induced by DGT demand. This suggests that, in this kind of sediment, DGT
465 measurement correctly reflects labile Cd from pore waters.

466 Our coupled biological approach, which included the confrontation of Cd accumulation rates
467 in DGT and bioaccumulation for 3 benthic organisms with different ecological life traits,
468 showed that *C. riparius* were exposed to a larger pool of Cd because they ingest particles.
469 Since Cd was mainly bound to the carbonate fraction, *C. riparius* were in fact able to desorb
470 Cd from carbonates. In contrast, Cd accumulation rates in *P. antipodarum* and DGT showed
471 the same slope, suggesting that *P. antipodarum* were exposed to pore waters only and that the
472 Cd pore waters labile fraction measured by DGT represented the bioavailable Cd fraction for
473 this species. Cd accumulation rates were the lowest for *G. fossarum*; hence, this species was
474 mainly influenced by Cd from overlaying waters. Our results are consistent with the known
475 behaviour of the 3 organisms.

476 Therefore, the proposed DGT technique proved its usefulness for sediment quality monitoring
477 and bioaccumulation prediction; nevertheless, its relevance for Cd and others metals would
478 need to be further assessed by testing DGT with a panel of sediments with contrasted
479 characteristics. Moreover, it might be more accurate, although more complex to apply, if

480 DGT measurement was realised on the whole sediment-water interface, in connection with
481 the living area of the studied species.

482

483 **Acknowledgements**

484

485 We gratefully acknowledge the following colleagues for sampling assistance, contribution to
486 field work and analytical support: Jean-Louis Roulier, Raphaël Mons, Lysiane Dherret,
487 Josiane Gahou, Eloise Vray, Bernard Motte and Rebecca Flück from Cemagref Lyon and
488 Bernard Loizeau from Forel Institute (Switzerland). This study was supported by a grant from
489 the French National Research Agency (ANR) in the framework of the “DIESE” program.

490

491 **References**

492

493 Allen HE, Fu G, Deng B. Analysis of acid-volatile sulfide (AVS) and simultaneously
494 extracted metals (SEM) for the estimation of potential toxicity in aquatic sediments.
495 *Environ Toxicol Chem* 1993; 12: 1441-1453.

496 Almås ÅR, Lombnæs P, Sogn TA, Mulder J. Speciation of Cd and Zn in contaminated soils
497 assessed by DGT-DIFS, and WHAM/Model VI in relation to uptake by spinach and
498 ryegrass. *Chemosphere* 2006; 62: 1647-1655.

499 Ankley GT. Evaluation of metal/acid-volatile sulfide relationships in the prediction of metal
500 bioaccumulation by benthic macroinvertebrates. *Environ Toxicol Chem* 1996; 15:
501 2138-2146.

502 Ankley GT, Mattson VR, Leonard EN, West CW, Bennett JL. Predicting the acute toxicity of
503 copper in freshwater sediments: Evaluation of the role of acid-volatile sulfide. *Environ*
504 *Toxicol Chem* 1993a; 12: 315-320.

505 Ankley GT, Liber K, Call DJ, Markee TP, Canfield TJ, Ingersoll CG. A field investigation of
506 the relationship between zinc and acid volatile sulfide concentrations in freshwater
507 sediments. *Journal of Aquatic Ecosystem Stress and Recovery* 1996; 5: 255-264.

508 Ankley GT, Benoit DA, Hoke RA, Leonard EN, West CW, Phipps GL, Mattson VR,
509 Anderson LA. Development and evaluation of test methods for benthic invertebrates
510 and sediments: Effects of flow rate and feeding on water quality and exposure
511 conditions. *Arch Environ Contam Toxicol* 1993b; 25: 12-19.

- 512 Baumann Z, Fisher NS. Relating the sediment phase speciation of arsenic, cadmium, and
513 chromium with their bioavailability for the deposit-feeding polychaete *Nereis*
514 *succinea*. *Environ Toxicol Chem* 2011; 30: 747-756.
- 515 Berry WJ, Hansen DJ, Mahony JD, Robson DL, Di Toro DM, Shipley BP, Rogers B, Corbin
516 JM, Boothman WS. Predicting the toxicity of metal-spiked laboratory sediments using
517 acid- volatile sulfide and interstitial water normalizations. *Environ Toxicol Chem*
518 1996; 15: 2067-2079.
- 519 Bervoets L, Blust R, De Wit M, Verheyen R. Relationships between river sediment
520 characteristics and trace metal concentrations in tubificid worms and chironomid
521 larvae. *Environ Pollut* 1997; 95: 345-356.
- 522 Buffle J, Wilkinson KJ, Stoll S, Filella M, Zhang J. A generalized description of aquatic
523 colloidal interactions: The three- colloidal component approach. *Environ Sci Technol*
524 1998; 32: 2887-2899.
- 525 Burton ED, Phillips IR, Hawker DW. Reactive sulfide relationships with trace metal
526 extractability in sediments from southern Moreton Bay, Australia. *Mar Pollut Bull*
527 2005; 50: 589-595.
- 528 Buykx SEJ, Bleijenberg M, Van den Hoop MAGT, Loch JPG. The effect of oxidation and
529 acidification on the speciation of heavy metals in sulfide-rich freshwater sediments
530 using a sequential extraction procedure. *J Environ Monitor* 2000; 2: 23-27.
- 531 Chapman AS, Foster IDL, Lees JA, Hodgkinson RJ, Jackson RH. Sediment and phosphorus
532 delivery from field to river via land drains in England and Wales. A risk assessment
533 using field and national databases. *Soil Use and Management* 2003; 19: 347-355.
- 534 Charbonneau P, Hare L, Carignan R. Use of x-ray images and a contrasting agent to study the
535 behavior of animals in soft sediments. *Limnol Oceanogr* 1998; 42: 1823-1828.
- 536 Chen Z, Mayer LM, Quetel C, Donard OFX, Self RFL, Jumars PA, Weston DP. High
537 concentrations of complexed metals in the guts of deposit feeders. *Limnol Oceanogr*
538 2000; 45: 1358-1367.
- 539 Cubillas P, Köhler S, Prieto M, Causserand C, Oelkers EH. How do mineral coatings affect
540 dissolution rates? An experimental study of coupled CaCO₃ dissolution - CdCO₃
541 precipitation. *Geochim Cosmochim Acta* 2005; 69: 5459-5476.
- 542 De Jonge M, Dreesen F, De Paepe J, Blust R, Bervoets L. Do acid volatile sulfides (AVS)
543 influence the accumulation of sediment-bound metals to benthic invertebrates under
544 natural field conditions? *Environ Sci Technol* 2009; 43: 4510-4516.

- 545 Di Toro DM, Mahony JD, Hansen DJ, Scott KJ, Carlson AR, Ankley GT. Acid volatile
546 sulfide predicts the acute toxicity of cadmium and nickel in sediments. *Environ Sci*
547 *Technol* 1992; 26: 96-101.
- 548 Ernstberger H, Davison W, Zhang H, Andrew TYE, Young S. Measurement and dynamic
549 modeling of trace metal mobilization in soils using DGT and DIFS. *Environ Sci*
550 *Technol* 2002; 36: 349-354.
- 551 Ernstberger H, Zhang H, Tye A, Young S, Davison W. Desorption kinetics of Cd, Zn, and Ni
552 measured in soils by DGT. *Environ Sci Technol* 2005; 39: 1591-1597.
- 553 Felten V, Charmantier G, Mons R, Geffard A, Rousselle P, Coquery M, Garric J, Geffard O.
554 Physiological and behavioural responses of *Gammarus pulex* (Crustacea: Amphipoda)
555 exposed to cadmium. *Aquat Toxicol* 2008; 86: 413-425.
- 556 Geffard A, Quéau H, Dedourge O, Biagianti-Risboug S, Geffard O. Influence of biotic and
557 abiotic factors on metallothionein level in *Gammarus pulex*. *Comparative*
558 *Biochemistry and Physiology - C Toxicology and Pharmacology* 2007; 145: 632-640.
- 559 Geffard O, Xuereb B, Chaumot A, Geffard A, Biagianti S, Noël C, Abbaci K, Garric J,
560 Charmantier G, Charmantier-Daures M. Ovarian cycle and embryonic development in
561 *Gammarus fossarum*: Application for reproductive toxicity assessment. *Environ*
562 *Toxicol Chem* 2010; 29: 2249-2259.
- 563 Gust M, Buronfosse T, Geffard O, Coquery M, Mons R, Abbaci K, Giamberini L, Garric J.
564 Comprehensive biological effects of a complex field poly-metallic pollution gradient
565 on the New Zealand mudsnail *Potamopyrgus antipodarum* (Gray). *Aquat Toxicol*
566 2011; 101: 100-108.
- 567 Harper MP, Davison W, Tych W. DIFS - A modelling and simulation tool for DGT induced
568 trace metal remobilisation in sediments and soils. *Environmental Modelling and*
569 *Software* 2000; 15: 55-66.
- 570 Hutchins CM, Teasdale PR, Lee J, Simpson SL. The effect of manipulating sediment pH on
571 the porewater chemistry of copper- and zinc-spiked sediments. *Chemosphere* 2007;
572 69: 1089-1099.
- 573 Komárek M, Zeman J. Dynamics of Cu, Zn, Cd, and Hg release from sediments at surface
574 conditions. *Bulletin of Geosciences* 2004; 79: 99-106.
- 575 Lacaze E, Devaux A, Mons R, Bony S, Garric J, Geffard A, Geffard O. DNA damage in
576 caged *Gammarus fossarum* amphipods: A tool for freshwater genotoxicity assessment.
577 *Environ Pollut* 2011; 159: 1682-1691.

- 578 Lee BG, Lee JS, Luoma SN, Choi HJ, Koh CH. Influence of acid volatile sulfide and metal
579 concentrations on metal bioavailability to marine invertebrates in contaminated
580 sediments. *Environ Sci Technol* 2000; 34: 4517-4523.
- 581 Lehto NJ, Sochaczewski Ł, Davison W, Tych W, Zhang H. Quantitative assessment of soil
582 parameter (KD and TC) estimation using DGT measurements and the 2D DIFS model.
583 *Chemosphere* 2008; 71: 795-801.
- 584 MacDonald DD, Ingersoll CG, Berger TA. Development and evaluation of consensus-based
585 sediment quality guidelines for freshwater ecosystems. *Arch Environ Contam Toxicol*
586 2000; 39: 20-31.
- 587 Mazurová E, Hilscherová K, Jálová V, Köhler HR, Triebkorn R, Giesy JP, Bláha L.
588 Endocrine effects of contaminated sediments on the freshwater snail *Potamopyrgus*
589 *antipodarum* in vivo and in the cell bioassays in vitro. *Aquat Toxicol* 2008; 89: 172-
590 179.
- 591 Mazurová E, Hilscherová K, Šídlová-Štěpánková T, Köhler H, Triebkorn R, Jungmann D,
592 Giesy JP, Bláha L. Chronic toxicity of contaminated sediments on reproduction and
593 histopathology of the crustacean *Gammarus fossarum* and relationship with the
594 chemical contamination and in vitro effects. *Journal of Soils and Sediments* 2010; 10:
595 423-433.
- 596 Michaut P. Données biologiques sur un Gastéropode Prosobranche récemment introduit en
597 Côte-d'Or, *Potamopyrgus jenkinsi*. *Hydrobiol* 1968; 32: 513-527.
- 598 Munkittrick KR, McCarty LS. An integrated approach to aquatic ecosystem health: top-down,
599 bottom-up or middle-out? *J Aquat Ecosyst Health* 1995; 4: 77-90.
- 600 Papadopoulos P, Rowell DL. The reactions of cadmium with calcium carbonate surfaces. *J*
601 *SOIL SCI* 1988; 39: 23-36.
- 602 Pellet B, Geffard O, Lacour C, Kermoal T, Gourlay-FrancÉ C, Tusseau-Vuillemin MH. A
603 model predicting waterborne cadmium bioaccumulation in *gammarus pulex*: the
604 effects of dissolved organic ligands, calcium, and temperature. *Environ Toxicol Chem*
605 2009; 28: 2434-2442.
- 606 Rachou J, Hendershot W, Sauvé S. Soil organic matter impacts upon fluxes of cadmium in
607 soils measured using diffusive gradients in thin films. *Communications in Soil Science*
608 *and Plant Analysis* 2007; 38: 1619-1636.
- 609 Roulier JL, Belaud S, Coquery M. Comparison of dynamic mobilization of Co, Cd and Pb in
610 sediments using DGT and metal mobility assessed by sequential extraction.
611 *Chemosphere* 2010; 79: 839-843.

- 612 Roulier JL, Tusseau-Vuillemin MH, Coquery M, Geffard O, Garric J. Measurement of
613 dynamic mobilization of trace metals in sediments using DGT and comparison with
614 bioaccumulation in *Chironomus riparius*: First results of an experimental study.
615 *Chemosphere* 2008; 70: 925-932.
- 616 Sañudo-Wilhelmy SA, Rossi FK, Bokuniewicz H, Paulsen RJ. Trace metal levels in
617 uncontaminated groundwater of a coastal watershed: Importance of colloidal forms.
618 *Environ Sci Technol* 2002; 36: 1435-1441.
- 619 Schmitt C, Balaam J, Leonards P, Brix R, Streck G, Tuikka A, Bervoets L, Brack W, van
620 Hattum B, Meire P, de Deckere E. Characterizing field sediments from three European
621 river basins with special emphasis on endocrine effects - A recommendation for
622 *Potamopyrgus antipodarum* as test organism. *Chemosphere* 2010; 80: 13-19.
- 623 Sochaczewski Ł, Tych W, Davison B, Zhang H. 2D DGT induced fluxes in sediments and
624 soils (2D DIFS). *Environmental Modelling and Software* 2007; 22: 14-23.
- 625 Tessier A, Campbell PGC, Blsson M. Sequential extraction procedure for the speciation of
626 particulate trace metals. *Anal Chem* 1979; 51: 844-851.
- 627 Thakur SK, Tomar NK, Pandeya SB. Influence of phosphate on cadmium sorption by calcium
628 carbonate. *Geoderma* 2006; 130: 240-249.
- 629 Vignati DAL, Dworak T, Ferrari B, Koukal B, Loizeau JL, Minouflet M, Camusso MI,
630 Polesello S, Dominik J. Assessment of the geochemical role of colloids and their
631 impact on contaminant toxicity in freshwaters: An example from the Lambro-Po
632 system (Italy). *Environ Sci Technol* 2005; 39: 489-497.
- 633 Warren LA, Tessier A, Hare L. Modelling cadmium accumulation by benthic invertebrates in
634 situ: The relative contributions of sediment and overlying water reservoirs to organism
635 cadmium concentrations. *Limnol Oceanogr* 1998; 43: 1442-1454.
- 636 Young LB, Harvey HH. Metal concentrations in chironomids in relation to the geochemical
637 characteristics of surficial sediments. *Arch Environ Contam Toxicol* 1991; 21: 202-
638 211.
- 639 Zhang H, Davison W. Performance characteristics of diffusion gradients in thin films for the
640 in situ measurement of trace metals in aqueous solution. *Anal Chem* 1995; 67: 3391-
641 3400.
- 642 Zhang H, Davison W. Direct in situ measurements of labile inorganic and organically bound
643 metal species in synthetic solutions and natural waters using diffusive gradients in thin
644 films. *Anal Chem* 2000; 72: 4447-4457.

645 Zhang H, Davison W, Miller S, Tych W. In situ high resolution measurements of fluxes of Ni,
646 Cu, Fe, and Mn and concentrations of Zn and Cd in porewaters by DGT. *Geochim*
647 *Cosmochim Acta* 1995; 59: 4181-4192.

648 Zhang H, Lombi E, Smolders E, McGrath S. Kinetics of Zn release in soils and prediction of
649 Zn concentration in plants using diffusive gradients in thin films. *Environ Sci Technol*
650 2004; 38: 3608-3613.

651 Zhang H, Zhao FJ, Sun B, Davison W, McGrath SP. A new method to measure effective soil
652 solution concentration predicts copper availability to plants. *Environ Sci Technol*
653 2001; 35: 2602-2607.

654

655

656

657

658

659

660

661

662

663

664

665

666

667

668

669

670

671

672

673

674

675

676

677

678

679 **Table captions**

680

681 Table 1: Physico-chemical characteristics and particulate trace metal concentrations of the
682 studied sediment. Cadmium concentrations in pore waters and in overlaying waters were
683 determined during the experiment.

684

685 Table 2: Partition coefficient (K_d) and parameters (K_{dl} : labile partition coefficient; T_c :
686 characteristic response time) deduced from 2D-DIFS modelling for the Control sediment and
687 the 3 highest Cd-spiked sediment concentrations.

688

689 Table 3: Concentrations of Cd bioaccumulated in *C. riparius*, *G. fossarum* and *P.*
690 *antipodarum*.

691

692 **Figure captions**

693

694 Fig. 1: (a) Mass of Cd accumulated in the DGT resin and (b) fluxes of Cd through the DGT as
695 a function of deployment time for the 3 highest Cd-spiked sediment concentrations (PG3.1,
696 PG7.8, PG19.5).

697

698 Fig. 2: (a) Cd concentrations in F2, F3 and F4 particulate fractions (mg kg^{-1}) and (b) relative
699 contributions (%) of the 3 fractions to total particulate Cd concentrations (for the Control
700 sediment and 3 highest Cd-spiked sediments PG3.1, PG7.8 and PG19.5).

701

702 Fig. 3: Bioaccumulation Cd rates (mean \pm sd, $n=3$) in *C. riparius*, *G. fossarum* and *P.*
703 *antipodarum* as a function of (a) total particulate Cd concentrations, (b) dissolved pore waters
704 Cd concentrations and (c) dissolved Cd concentration in overlaying waters. Accumulation Cd
705 rates in DGT after 144 hours of deployment are reported for the 3 highest Cd-spiked sediment
706 concentrations (d).

707

708 Fig 4: Distribution of the R ratio for sediments Cd-spiked at 3.1, 7.8 and 19.5 mg kg^{-1} .

709

710 Fig. 5: Cadmium concentrations in *C. riparius* as a function of particulate Cd concentrations
711 for (●) this study and for (○) the study of Roulier et al. (2008).

712

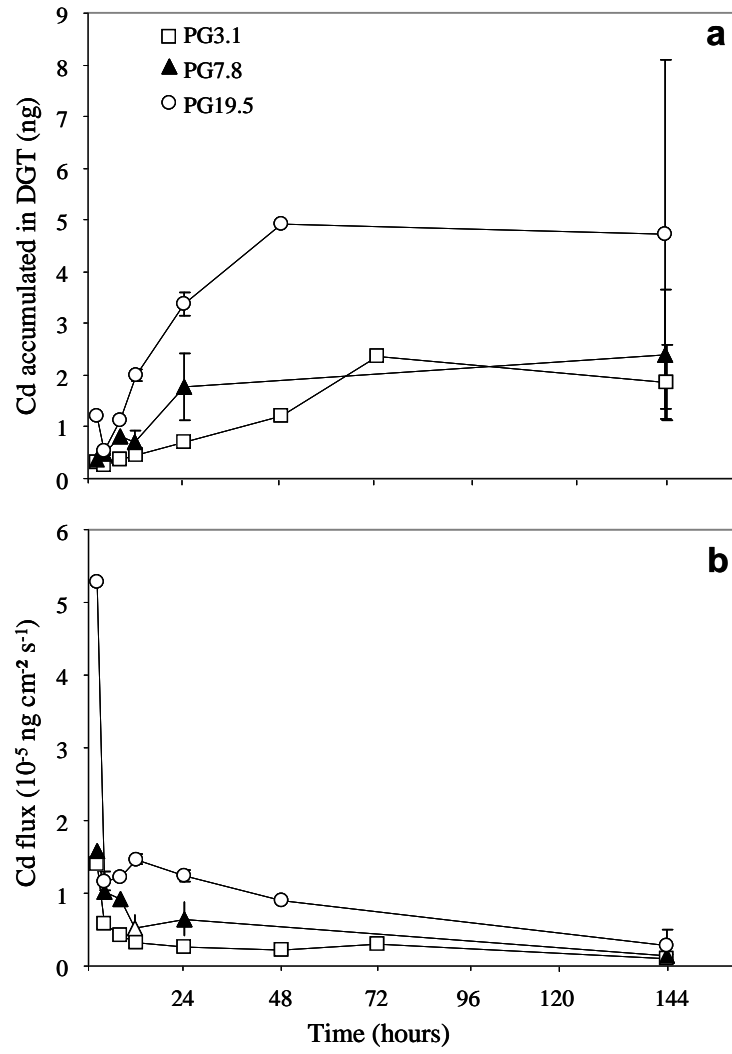


Fig. 1.

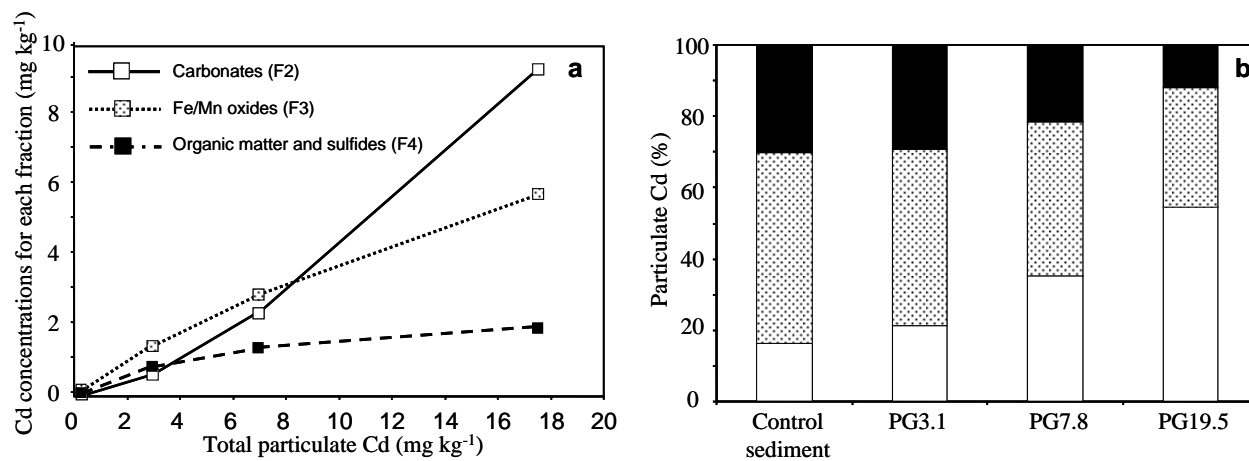


Fig. 2.

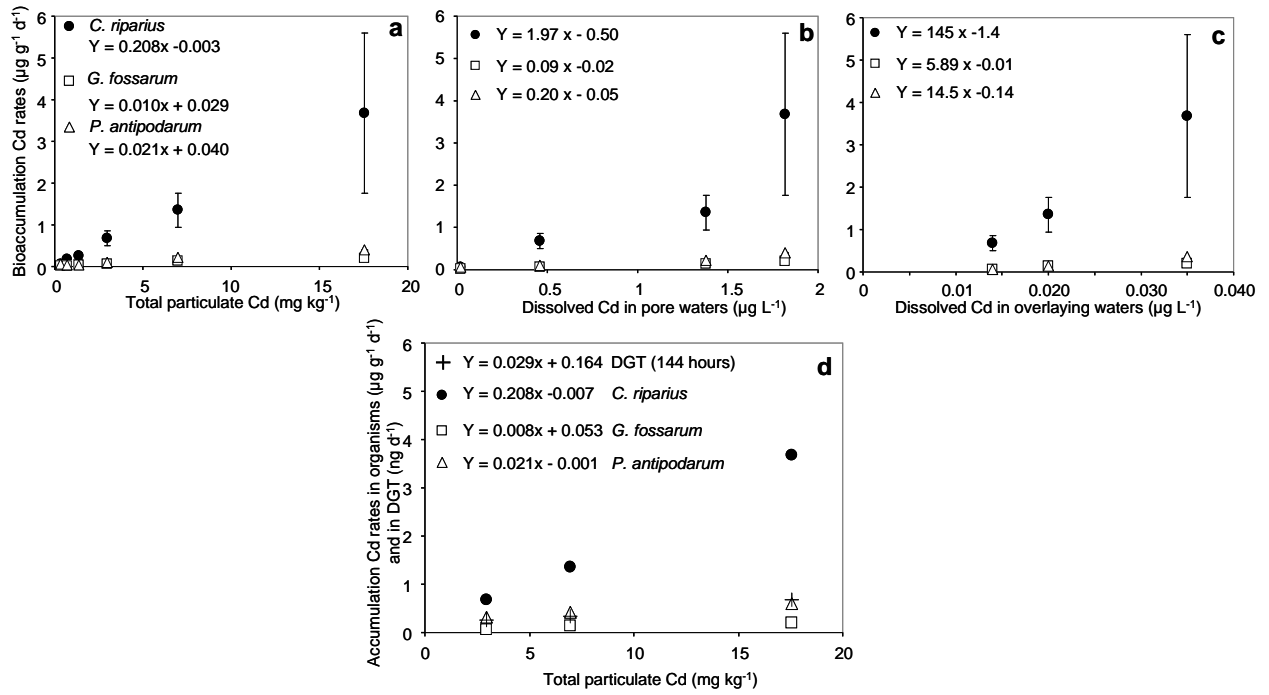


Fig. 3:

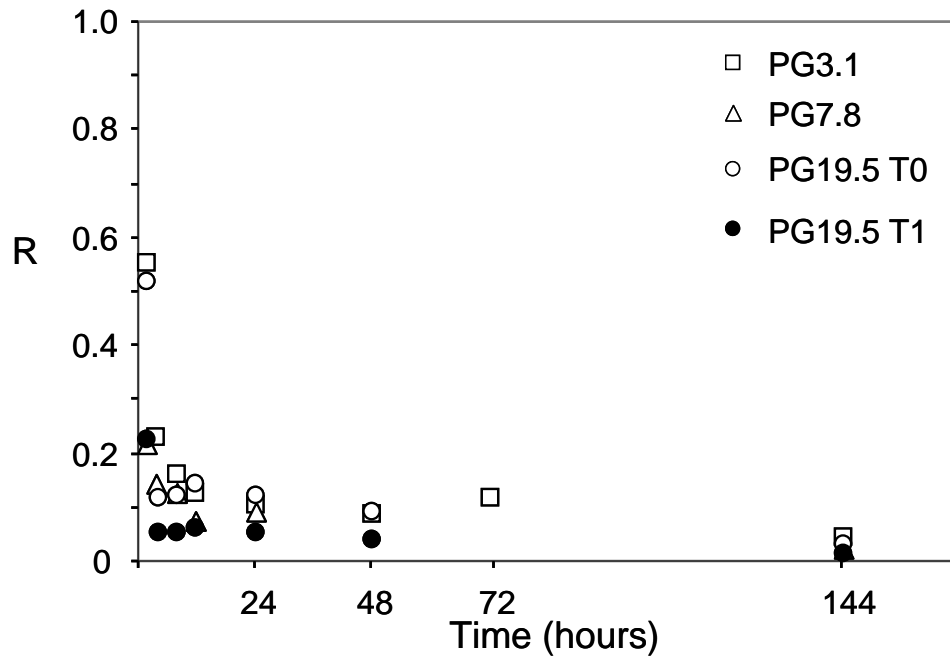


Fig 4:

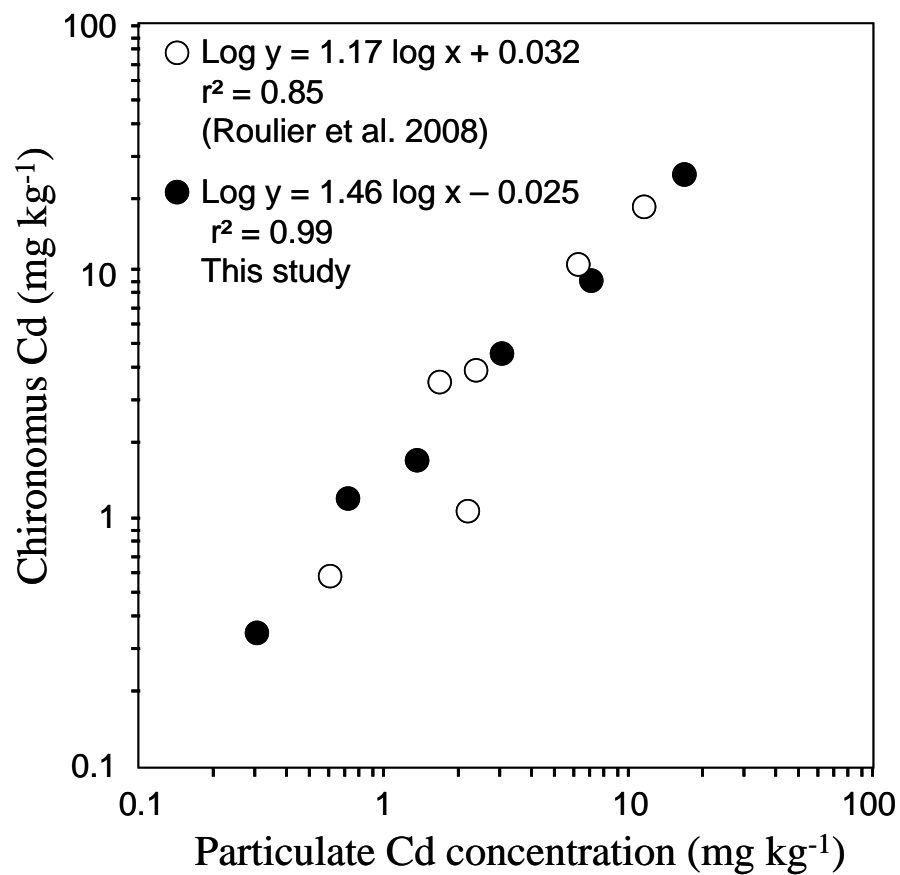


Fig. 5: